

# Analyst

Accepted Manuscript



This is an *Accepted Manuscript*, which has been through the Royal Society of Chemistry peer review process and has been accepted for publication.

*Accepted Manuscripts* are published online shortly after acceptance, before technical editing, formatting and proof reading. Using this free service, authors can make their results available to the community, in citable form, before we publish the edited article. We will replace this *Accepted Manuscript* with the edited and formatted *Advance Article* as soon as it is available.

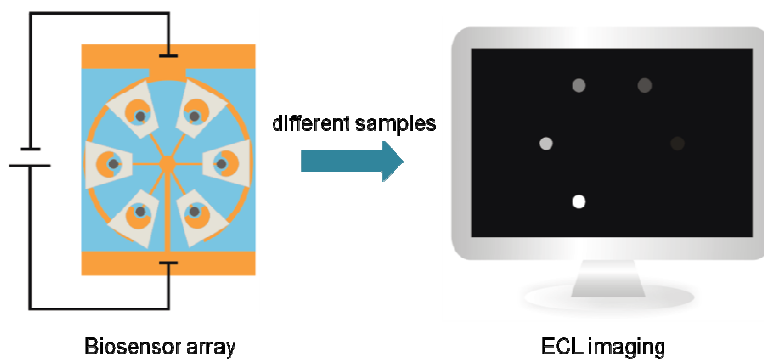
You can find more information about *Accepted Manuscripts* in the [Information for Authors](#).

Please note that technical editing may introduce minor changes to the text and/or graphics, which may alter content. The journal's standard [Terms & Conditions](#) and the [Ethical guidelines](#) still apply. In no event shall the Royal Society of Chemistry be held responsible for any errors or omissions in this *Accepted Manuscript* or any consequences arising from the use of any information it contains.

# A Novel Biosensor Array with a Wheel-like Pattern for Glucose, Lactate and Choline Based on Electrochemiluminescence Imaging

Zhenyu Zhou, Linru Xu, Suozhu Wu, Bin Su\*

An ECL imaging biosensor was fabricated for detecting glucose, lactate and choline, as well as simultaneous multicomponent assay.



Cite this: DOI: 10.1039/c0xx00000x

www.rsc.org/xxxxxx

ARTICLE TYPE

# A Novel Biosensor Array with a Wheel-like Pattern for Glucose, Lactate and Choline Based on Electrochemiluminescence Imaging

Zhenyu Zhou,<sup>a</sup> Linru Xu,<sup>a</sup> Suozhu Wu<sup>b</sup> and Bin Su<sup>\*a</sup>

Received (in XXX, XXX) Xth XXXXXXXXXX 20XX, Accepted Xth XXXXXXXXXX 20XX

DOI: 10.1039/b000000x

Electrochemiluminescence (ECL) imaging provides a superior approach to achieve array detection because of its ability for ultrasensitive multiplex analysis. In this paper, we reported a novel ECL imaging biosensor array modified with enzyme/carbon nanotubes/chitosan composite film for the determination of glucose, choline and lactate. The biosensor array was constructed by integrating a patterned indium tin oxide (ITO) glass plate with six perforated poly(dimethylsioxane) (PDMS) covers. ECL is generated by the electrochemical reaction between luminol and hydrogen peroxide that is produced by enzyme catalysed oxidation of different substrates with molecular oxygen, and ECL images were captured by a charge-coupled device (CCD) camera. The separated electrochemical micro-cells enabled a simultaneous assay of six samples at different concentrations. From the established calibration curves, the detection limits were 14  $\mu\text{M}$  for glucose, 40  $\mu\text{M}$  for lactate and 97  $\mu\text{M}$  for choline, respectively. Moreover, multicomponent assays and cross reactivity were also studied, both of which were satisfied for analysis. This biosensing platform based on ECL imaging shows many distinct advantages, including miniaturization, low cost, and multi-functionalization. We believe that it has potential applications in clinical diagnosis, medicine and food inspection.

## Introduction

Electrochemiluminescence (ECL), known as a powerful and attractive method of detection, can be defined as chemiluminescence (CL) initiated and manipulated by electrochemistry.<sup>1</sup> It possesses the intrinsic advantages of both electrochemistry and CL, including simplicity, high sensitivity, low cost and wide dynamic range.<sup>2</sup> In addition, ECL allows both temporal and spatial control, and simultaneously collection of two parameters (light intensity and current) versus potential,<sup>3,4</sup> leading a great selectivity and controllability over the reaction. Consequently, it has received significant attention in analytical chemistry and clinical diagnostics in recent years.<sup>2,5,6</sup> So far, all commercially available ECL analytical instruments are based on coreactant ECL technology<sup>5</sup> which includes two primary systems, i.e., ruthenium complex with amine-containing compounds as coreactants<sup>7-9</sup> or a luminol-H<sub>2</sub>O<sub>2</sub> system.<sup>10</sup>

ECL signals can be collected by a photomultiplier tube (PMT) and a CCD camera alternatively. Even though most of the ECL analysis utilize the former to achieve high sensitivity and a low detection limit, ECL imaging (generally recorded by a CCD) offers remarkable superiorities over ECL intensity (recorded by a PMT), in particular for high-throughput analysis.<sup>11,12</sup> Furthermore, ECL imaging can be measured with a mobile camera phone,<sup>13</sup> or even naked eyes,<sup>14</sup> without complicated detecting systems and time-consuming data processing. Over the past two decades, ECL imaging has been extensively investigated and applied in various areas, including the metabolic toxicity screening,<sup>12,15</sup> immunoassay,<sup>16,17</sup> latent fingerprints visualization,<sup>18,19</sup> inorganic

and biological compounds testing,<sup>20,21</sup> electron-transfer kinetics,<sup>22</sup> and microfluidic system with bipolar electrodes.<sup>23</sup>

Glucose is widely distributed in the human body, and a significant fluctuation of blood glucose levels in diabetics can cause serious complications.<sup>24</sup> Lactate is a key product in the anaerobic glycolytic pathway, which also has found applications in food and pharmaceuticals.<sup>25,26</sup> Choline is found in many organs, and is the precursor molecule for acetylcholine which involved in memory and muscle control.<sup>27</sup> Consequently, detection of the three biomolecules has great value in diagnostic assay, medicine and food inspection. Electroanalytical methods based on the amperometric enzyme technology play a leading role in measuring the concentrations of these species,<sup>28-32</sup> however, the challenges still remain because of interference from coexisting electroactive compounds and incompatibility of multiplexed assays. Marquette and coworkers addressed these two issues by introducing an elegant ECL imaging approach.<sup>33,34</sup> Different oxidases specific to the biomolecules were non-covalently immobilized on Sepharose beads, embedded in poly(vinyl alcohol) bearing styryl-pyridinium groups (PVA-SbQ) photopolymer, and then spotted on the surface of a glass carbon foil. On the basis of a similar entrapment concept, they have also presented another multi-parametric ECL biochip by entrapping two oxidases on a screen-printed graphite electrode microarray.<sup>35</sup> Unfortunately, these sensing platforms suffered from complicated enzyme immobilization or adopting a sophisticated device. Herein we developed a novel ECL imaging biosensor array to accomplish the analysis of glucose, choline and lactate. The biosensor array

was fabricated by integrating a patterned indium tin oxide (ITO) glass plate with six perforated poly(dimethylsiloxane) (PDMS) covers. Carbon nanotubes have been considered as an attractive material and often used to fabricate electrochemical sensors because of their unique properties including flexibility, chemical stability and high electrical conductivity.<sup>36,37</sup> It was aligned with chitosan, a natural biopolymer with excellent film-forming ability and high mechanical strength,<sup>38,39</sup> to entrap enzymes in order to keep high activity and good stability.<sup>40</sup> After microliter-sized liquid droplets containing luminol and substrates were loaded into micro-cells, the ECL reaction between enzymatically generated hydrogen peroxide (H<sub>2</sub>O<sub>2</sub>) and luminol can occur under an appropriate externally applied potential. Multiple optical signals from micro-cells could be captured by a CCD camera. This ECL imaging-based biosensor array showed a satisfying performance for detecting of the three biomolecules, as well as simultaneous multicomponent assays in complex samples.

## Experimental

### Chemicals and materials

All chemicals of analytical reagent grade were used as received without further purification. Luminol, choline chloride and chitosan (CS, >95% deacetylation, MW  $\sim 1 \times 10^6$ ) were bought from Aladdin Chemical Reagents. Choline oxidase (COD, EC 1.1.3.17, from *Alcaligenes species*,  $\geq 10$  U mg<sup>-1</sup>), lactate oxidase (LOD, EC 1.13.12.4, from *Pediococcus species*,  $\geq 20$  U mg<sup>-1</sup>) and L-(+)-lactate lithium salt (96%) were obtained from Sigma-Aldrich. Glucose oxidase (GOD, >100 U mg<sup>-1</sup>) was purchased from Sangon Biotech Co. Ltd. Multiwall carbon nanotubes (MWCNTs) were bought from Nanjing XF NANO Materials Tech Co. Ltd. Glucose was received from Sinopharm Chemical Reagent Co. Ltd. 0.1 M phosphate buffer solution (PBS, pH 7.4) containing 0.15 M NaCl was prepared as the supporting electrolyte. PDMS and curing agent were purchased from Dow Corning (Midland, MI, USA). Positive photoresist AZ-P4620 was

ITO coated glasses (ITO thickness:  $\sim 100$  nm, resistance: <15  $\Omega$ /square) were bought from Kaivo Electronic Components Co., Ltd (Zhuhai, China). Prior to use, the ITO glass was washed sequentially in acetone, ethanol and ultrapure water by sonication (each for 15 min).

### Fabrication of the hybrid materials of enzymes, MWCNTs and CS

The hybrid GOD/MWCNTs/CS solution was prepared as previously described by Liu et al.<sup>40</sup> Briefly, a 10 mg mL<sup>-1</sup> CS solution was prepared by dissolving CS powder in 1% (v/v) acetate acid with ultrasonication for ca. 40 min. Then 4 mg of MWCNTs was dispersed in 2 mL of CS solution under ultrasonic agitation, resulting in a viscous and black suspension. Next, 200  $\mu$ L of the resultant suspension was mixed thoroughly with 100  $\mu$ L of GOD solution (5 mg mL<sup>-1</sup>, 0.1 M PBS). The COD/MWCNTs/CS and LOD/MWCNTs/CS mixtures were prepared in a similar way, except that the pH of CS solution was adjusted to 5.0 with a 0.1 M NaOH solution, and the final concentration of COD and LOD was 1 mg mL<sup>-1</sup>.

### Fabrication of GOD/MWCNTs/CS/ITO electrodes

20  $\mu$ L of the mixture containing GOD/MWCNTs/CS prepared as aforementioned was pipetted on an ITO glass chip (available area: 1.2 cm  $\times$  2.5 cm) and spread over the surface. Finally, the modified ITO electrode was allowed to dry at 4  $^{\circ}$ C overnight to achieve a robust film containing GOD/MWCNTs/CS.

### Fabrication of the biosensor array

The biosensor array consisted of PDMS covers and an ITO glass plate with a wheel-like pattern. The PDMS covers were prepared according to a previous report.<sup>41</sup> Briefly, PDMS monomer and its curing agent were uniformly blended with a ratio of 10:1 (w/w), and degassed in a closed container connected to a vacuum pump for 30 min. The solution was poured onto a glass mold and baked on a hot plate at 75  $^{\circ}$ C for 1.5 h. A slice of PDMS was then peeled off and cut into small pieces, on which holes (6 mm in

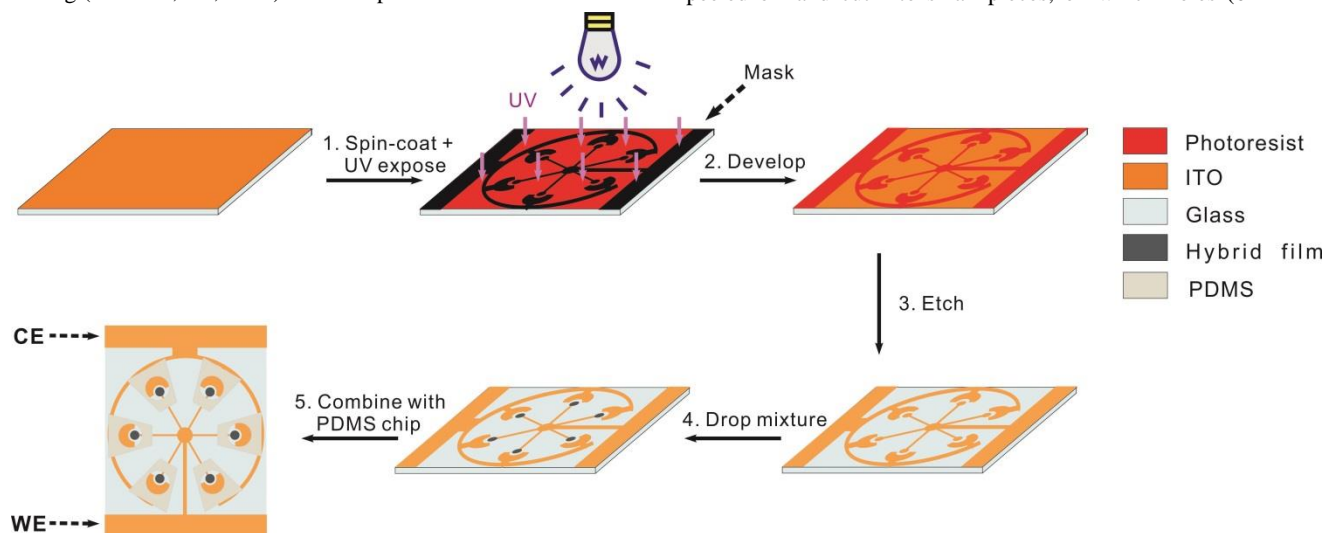


Fig. 1 Schematic procedure for fabrication of the biosensor array.

bought from Clariant (Somerville, NJ, USA). Ultrapure water (18.2 M $\Omega$  cm) purified by a Millipore system was used throughout the experiment.

diameter) were drilled for holding substrate solutions. The average thickness of the PDMS cover was 3 mm.

The photolithographic technique and chemical etching were

employed to pattern the ITO glass plate, as shown in Fig. 1.<sup>20</sup> First, an ITO glass substrate (4 cm × 5 cm) was spin-coated with a layer of positive photoresist (thickness: ~10 μm), followed by curing in an oven at 110 °C for 3 min. Then the photoresist layer was patterned by covering a photomask under UV irradiation (365 nm, JKG-2A lithographic device, Photomechanical Co. Shanghai, China). After being developed with a 0.7% NaOH solution, the ITO glass plate was heated for another 30 min at 110 °C. Subsequently, the unmasked portion of the ITO layer was removed by wet etching in an acid solution (HNO<sub>3</sub>/HCl/H<sub>2</sub>O = 4:5:5, v/v/v), and the photoresist was cleaned up with acetone. Then, 1 μL of GOD/MWCNTs/CS (LOD/MWCNTs/CS or COD/MWCNTs/CS) hybrid solution was carefully spotted onto each disk working electrode.

Finally, PDMS covers with small holes were combined tightly to the patterned ITO glass plate after being treated with air plasma for ~25 s. The biosensor array chip was stored at 4 °C when not in use.

### Electrochemical characterization and ECL measurements

Electrochemical measurements of the GOD/MWCNTs/CS/ITO electrode were performed on a CHI 832 electrochemical analysis station (CH Instrument, Shanghai) with a traditional three-electrode system. A piece of modified or bare ITO glass chip (fixed area: ~0.13 cm<sup>2</sup>) was served as the working electrode, with a platinum wire and a KCl-saturated Ag/AgCl electrode as the auxiliary and reference electrode, respectively. ECL intensity versus potential was measured by a MPI-E ECL analytical system (PMT voltage: 600 V, Remex Analysis Instrument, Xi'an, China).

The ECL images were acquired by a CCD camera (Model Clix Clx210) equipped with a Model VFA2595H Macro Zoom Iris Megapixel lens (Senko ADL, Japan) with an exposure time of 1 min. The ECL reaction on the biosensor array was triggered by applying a constant potential of 2.0 V at two ends of the ITO plate. The gray value analysis of CCD images was done using the ImageJ software.

## Results and discussion

### Electrochemical and electrochemiluminescent properties of the GOD/MWCNTs/CS hybrid film

The electrochemical properties of ITO electrodes with different surface modification were studied by cyclic voltammetry (CV) in an aqueous solution containing ferri/ferrocyanide redox couple, as shown in Fig. 2A. It can be seen that the current magnitude of CS covered ITO electrode (curve b) is larger than that of the bare ITO electrode (curve a), which can be ascribed to electrostatically attractive interaction between the redox probe [Fe(CN)<sub>6</sub>]<sup>3-/4-</sup> and protonated amino groups of CS film.<sup>42</sup> When MWCNTs was added to the CS matrix, a further increase in the peak current was observed due to its good conductivity (curve c). However, the electrochemical response was suppressed after GOD molecules were added (curve d), suggesting that GOD molecules served as an inert electron and mass-transfer blocking units.

Fig. 2B compares the gray values of ECL images obtained for different modified electrodes biased at a constant potential of 0.8 V. A pretty weak optical signal was recorded at the bare ITO electrode due to the background ECL of luminol. When CS or MWCNTs/CS film was assembled on the ITO electrode surface,

the ECL intensity decreased apparently. It is reasonable since the CS matrix might act as a barrier hindering the diffusion of luminol to the surface of the underlying electrode. In contrast, after GOD was added to the MWCNTs/CS composite, the ECL intensity increased apparently, indicating that hydrogen peroxide was enzymatically generated by GOD to promote the ECL of luminol. A 60% decrease of gray value was observed on the GOD/CS/ITO electrode compared to the GOD/MWCNTs/CS/ITO electrode, indicating that MWCNTs can facilitate the electron transfer and enhance the ECL intensity.

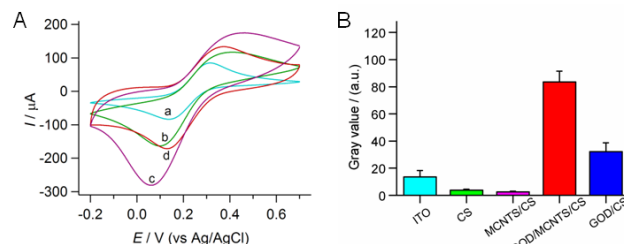


Fig. 2 (A) CVs of different electrodes in 0.1 M PBS (pH 7.4) containing 2 mM [Fe(CN)<sub>6</sub>]<sup>3-/4-</sup>: bare ITO (a), CS/ITO (b), MWCNTs/CS/ITO (c) and GOD/MWCNTs/CS/ITO (d). The scan rate was 0.1 V s<sup>-1</sup>. (B) The ECL image gray values of different electrodes biased at a constant potential of 0.8 V in 0.1 M PBS (pH 7.4) containing 1.3 mM luminol and 1 mM glucose.

### Optimized conditions for the GOD/MWCNTs/CS/ITO chip

The concentration of luminol was optimized on an ITO electrode modified with GOD/MWCNTs/CS hybrid film. Fig. 3 shows the ECL intensities of the luminol-glucose mixtures with different volume ratios, from which we can see that the ECL intensity increased rapidly with the content of luminol before saturating at a volume ratio of 0.15 (blue). Meanwhile, luminol is nearly non-luminescent when dissolved in PBS without glucose (red). Furthermore, the control experiment without applying an external voltage indicates that the contribution of CL to the overall luminescence intensity can be also neglected (see Fig. S1). Therefore, 0.15 was selected as the optimal volume ratio of luminol solution to the substrate solution.

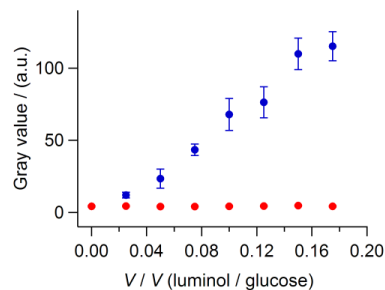
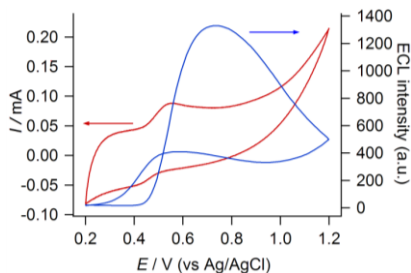


Fig. 3 The effect of volume ratio of luminol versus glucose on the gray value of the ECL image in 0.1 M PBS with (blue) or without (red) glucose. The concentrations of luminol and glucose solutions are 10 mM and 1 mM, respectively.

In addition, it is important to apply a suitable potential in order to facilitate the sensitivity of this approach. The ECL-voltage curve with corresponding cyclic voltammogram of a PBS solution containing glucose and luminol was measured in the potential range from 0.2 V to 1.2 V vs. Ag/AgCl (Fig. 4). An

apparent oxidation peak can be found at ca. 0.5 V (red line), corresponding to the oxidation of luminol to a radical anion at the surface of the GOD/MWCNTs/CS-modified ITO electrode.<sup>4</sup> However, the maximum ECL emission occurred at potential of 0.8 V, as seen from the ECL-voltage curve (blue line). Therefore, 0.8 V was applied for the following ECL imaging experiments on the GOD/MWCNTs/CS/ITO electrode.



**Fig. 4** CV (red line) and ECL-voltage curves (blue line) recorded in 0.1 M PBS (pH 7.4) containing 1.3 mM luminol and 1 mM glucose with the GOD/MWCNTs/CS/ITO electrode. The scan rate was 100 mV s<sup>-1</sup>.

### Quantitative detection of glucose on the GOD/MWCNTs/CS/ITO chip

Under the optimized conditions, ECL images of the GOD/MWCNTs/CS/ITO electrode were recorded in solutions containing different concentrations of glucose. By analyzing the gray value in each digital image, it is clear that the ECL intensity increased sharply with the concentration of glucose, and reached a plateau at a concentration higher than 5 mM (see Fig 5). The calibration curve displayed a good linear relationship between gray value of ECL images and the glucose concentration in the range from 0.05 to 2 mM with the regression equation of  $G = 6.4563 + 68.348 [\text{glucose}] \text{ (mM)}$  ( $n = 6, R = 0.9957$ ), where  $G$  is the gray value of ECL images. The detection limit of the substrate was found to be 5 μM, which was calculated as the blank value plus three times the standard deviation.

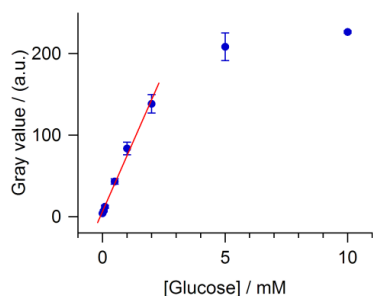


**Fig. 5** Calibration curve for glucose detection using the GOD/MWCNTs/CS/ITO electrode in 0.1 M PBS (pH 7.4) containing 1.3 mM luminol.

### Quantitative detection of glucose, choline and lactate on the biosensor array

A biosensor array composed of six working electrodes covered with oxidase/MWCNTs/CS hybrid films was employed to detect different concentrations of biomolecules simultaneously. Before applying a proper voltage, 30 μL of aqueous droplets containing various concentrations of one substrate were counterclockwise introduced into micro-cells with a microsyringe (from 1 to 6 in Fig. 6A). Here taking glucose as an example, ECL signals were

spatially localized at the surface of the working electrode array. Moreover, thanks to the sufficient distance between two micro-cells, ECL signals would not be disturbed by the adjacent one, hence improving the accuracy. As seen in Fig 6A and 6B, the gray value of spots increased proportionally with the glucose concentration, and a linear response to concentration was observed between 0.02 mM and 2 mM (Fig. 6C). The regression equation can be described as  $G = -0.8035 + 105.76 [\text{glucose}] \text{ (mM)}$  ( $n = 6, R = 0.9944$ ) with a detection limit of 14 μM (S/N = 3). Importantly, the blank was undetectable under the experimental condition, thus a lower detection limit may be achievable with a longer exposure time.

This device was also applied to determine choline chloride and lactate (details in EIS†, Fig. S-2, Fig. S-3 and Table S-1). From the constructed calibration curves, the detection limits of choline chloride and lactate were 40 μM and 97 μM, respectively.

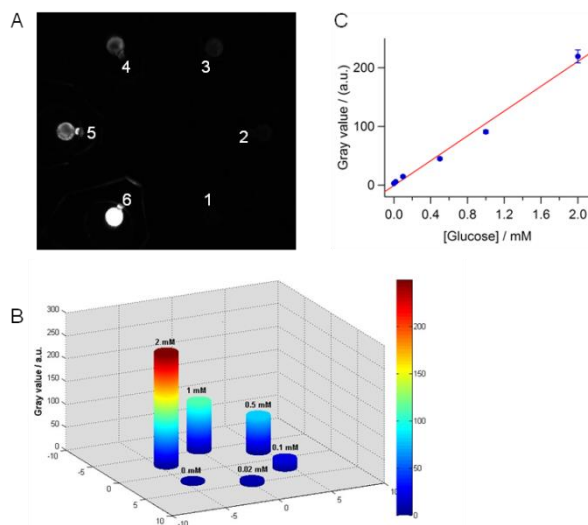


**Fig. 6** (A) An ECL image of the biosensor array for different concentrations of glucose (1-6: 0 mM, 0.02 mM, 0.1 mM, 0.5 mM, 1 mM, 2 mM); (B) The corresponding 3D-ECL image of (A); (C) Linear relationship between gray value of ECL spots and the glucose concentration. The solution was 0.1 M PBS (pH 7.4) containing 1.3 mM luminol.

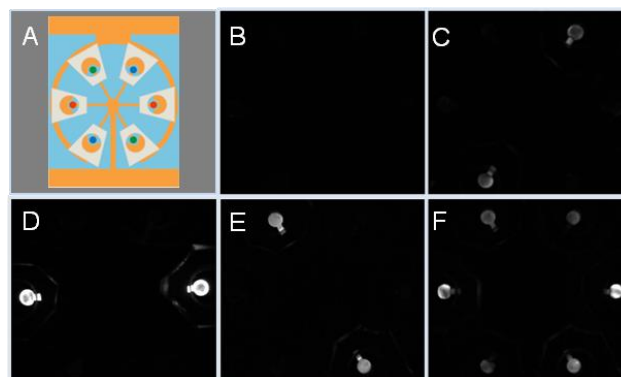


**Fig. 7** (A) Illustration of the biosensor array with COD (blue spots), GOD (green spots) and LOD (red spots) diagonally immobilized on the working electrodes. ECL images captured for a blank solution (B) and solutions containing 1 mM choline chloride (C), 2 mM lactate (D), 1 mM glucose (E), and a mixture containing choline chloride, glucose and lactate all at a concentration of 1 mM (F). The solution was 0.1 M PBS (pH 7.4) containing 1.3 mM luminol.

## Cross reactivity evaluation and simultaneous multianalyte detection on the biosensor array

To validate the resistance to the cross-talk, the cross-reactivity between enzymes and biological compounds was studied. For this purpose, three different oxidases (COD, GOD and LOD) were immobilized diagonally onto six working electrodes of one biosensor array (Fig. 7A). The performance was evaluated by comparing the ECL images captured when the PDMS micro-cells were all filled with a blank solution, choline chloride, glucose, or lactate solution. As expected, no light emission was generated with the blank solution, meanwhile, precisely localized ECL signals could only be observed on the working electrodes modified with the corresponding oxidase (Fig. 7B-E).

It is well-known that the simultaneous detection of a complex solution composed of multiple targets has a high practical significance. When a mixture containing three substrates (choline chloride, glucose and lactate) was tested on this biosensor array, as processed in Fig. 7A, three couples of working electrodes were lighted up with different ECL intensities (Fig. 7F). The measured concentrations of three substrates (calculated by the corresponding regression equations) were  $1.013 \pm 0.048$  mM (choline chloride),  $1.016 \pm 0.137$  mM (glucose) and  $0.985 \pm 0.077$  mM (lactate), which reached good agreement with the standard value, namely 1 mM.

## Conclusion

A flexible ECL imaging biosensor array based on the reaction of luminol and enzymatically generated hydrogen peroxide was proposed in this work. By assembling six PDMS covers and a processed ITO plate, the biosensing platform was fabricated, and employed to detect choline chloride, glucose and lactate. The results showed a good linear relationship between the gray value of ECL images and the concentration of each substrate. When different types of oxidases were separately modified on the electrodes, multianalyte solutions could be determined without cross-contamination. This biosensing platform processes advantages of low cost, low-voltage DC power supply and high throughput. Moreover, immunoassay can be accomplished by immobilizing antigens or antibodies on MWCNTs/CS/ITO working electrodes via the cross-linking reaction.<sup>43</sup> A larger scaled array encompassing tens or even hundreds of electrodes will be also feasible if the size of the PDMS covers and the geometries of the electrodes can be fabricated properly. We believe that this ECL biosensing array has potential applications in clinical diagnosis, medicine and food inspection.

## Acknowledgements

This research is supported by the National Nature Science Foundation of China (21222504, 21335001), the Program for New Century Excellent Talents in University and the Fundamental Research Funds for the Central Universities (2014XZZX003-04).

## Notes and references

<sup>a</sup> Institute of Microanalytical Systems, Department of Chemistry, Zhejiang University, Hangzhou 310058, China. Fax: +86 571-88273572; Tel: +86 571-88273496; E-mail: subin@zju.edu.cn

<sup>b</sup> College of Food Science and Engineering, Shanxi Agricultural University, Taigu 030801, China.

† Electronic Supplementary Information (ESI) available: Fig.S-1, Fig.S-2, Fig.S-3 and Table S-1. See DOI: 10.1039/b000000x/

1. H. Dai, X. Wu, H. Xu, Y. Wang, Y. Chi and G. Chen, *Electrochim. Acta*, 2009, **54**, 4582-4586.
2. M. M. Richter, *Chem. Rev.*, 2004, **104**, 3003-3036.
3. H. Zhou, S. Kasai and T. Matsue, *Anal. Biochem.*, 2001, **290**, 83-88.
4. R. Lei, L. Stratmann, D. Schafer, T. Erichsen, S. Neugebauer, N. Li and W. Schuhmann, *Anal. Chem.*, 2009, **81**, 5070-5074.
5. W. J. Miao, *Chem. Rev.*, 2008, **108**, 2506-2553.
6. L. Hu and G. Xu, *Chem. Soc. Rev.*, 2010, **39**, 3275-3304.
7. J. Li, Q. Yan, Y. Gao and H. Ju, *Anal. Chem.*, 2006, **78**, 2694-2699.
8. W. Zhan and A. J. Bard, *Anal. Chem.*, 2007, **79**, 459-463.
9. X. Zhang, C. Chen, J. Li, L. Zhang and E. Wang, *Anal. Chem.*, 2013, **85**, 5335-5339.
10. Y. Cao, R. Yuan, Y. Chai, L. Mao, H. Niu, H. Liu and Y. Zhuo, *Biosens. Bioelectron.*, 2012, **31**, 305-309.
11. K.-F. Chow, F. Mavre, J. A. Crooks, B.-Y. Chang and R. M. Crooks, *J. Am. Chem. Soc.*, 2009, **131**, 8364-8365.
12. D. P. Wasalathanthri, S. Malla, I. Bist, C. K. Tang, R. C. Faria and J. F. Rusling, *Lab Chip*, 2013, **13**, 4554-4562.
13. J. L. Delaney, C. F. Hogan, J. Tian and W. Shen, *Anal. Chem.*, 2011, **83**, 1300-1306.
14. Z.-j. Lin, X.-m. Chen, T.-t. Jia, X.-d. Wang, Z.-x. Xie, M. Oyama and X. Chen, *Anal. Chem.*, 2009, **81**, 830-833.
15. E. G. Hvastkovs, M. So, S. Krishnan, B. Bajrami, M. Tarun, I. Jansson, J. B. Schenkman and J. F. Rusling, *Anal. Chem.*, 2007, **79**, 1897-1906.
16. F. Deiss, C. N. LaFratta, M. Symer, T. M. Blicharz, N. Sojic and D. R. Walt, *J. Am. Chem. Soc.*, 2009, **131**, 6088-6089.
17. N. P. Sardesai, J. C. Barron and J. F. Rusling, *Anal. Chem.*, 2011, **83**, 6698-6703.
18. L. Xu, Y. Li, S. Wu, X. Liu and B. Su, *Angew. Chem., Int. Ed.*, 2012, **124**, 8192-8196.
19. L. Xu, Y. Li, Y. He and B. Su, *Analyst*, 2013, **138**, 2357-2362.
20. S. Wu, Z. Zhou, L. Xu, B. Su and Q. Fang, *Biosens. Bioelectron.*, 2014, **53**, 148-153.
21. A. Chovin, P. Garrigue and N. Sojic, *Bioelectrochemistry*, 2006, **69**, 25-33.
22. Y.-L. Chang, R. E. Palacios, F.-R. F. Fan, A. J. Bard and P. F. Barbara, *J. Am. Chem. Soc.*, 2008, **130**, 8906-8907.
23. M.-S. Wu, D.-J. Yuan, J.-J. Xu and H.-Y. Chen, *Chem. Sci.*, 2013, **4**, 1182-1188.
24. S. P. Nichols, A. Koh, W. L. Storm, J. H. Shin and M. H. Schoenfish, *Chem. Rev.*, 2013, **113**, 2528-2549.
25. B. Haghighi and S. Bozorgzadeh, *Talanta*, 2011, **85**, 2189-2193.
26. P. i. Mäki-Arvela, I. L. Simakova, T. Salmi and D. Y. Murzin, *Chem. Rev.*, 2013.
27. V. C. Tsafack, C. A. Marquette, F. Pizzolato and L. c. J. Blum, *Biosens. Bioelectron.*, 2000, **15**, 125-133.
28. T. Yao, *Anal. Chim. Acta*, 1983, **153**, 169-174.
29. F. L. Qu, M. H. Yang, J. H. Jiang, G. L. Shen and R. Q. Yu, *Anal. Biochem.*, 2005, **344**, 108-114.
30. C.-L. Lin, C.-L. Shih and L.-K. Chau, *Anal. Chem.*, 2007, **79**, 3757-3763.
31. E. I. Yashina, A. V. Borisova, E. E. Karyakina, O. I. Shchegolikhina, M. Y. Vagin, D. A. Sakharov, A. G. Tonevitsky and A. A. Karyakin, *Anal. Chem.*, 2010, **82**, 1601-1604.
32. J. Wang, *Chem. Rev.*, 2008, **108**, 814-825.
33. C. Marquette and L. Blum, *Sens. Actuators, B*, 2003, **90**, 112-117.
34. C. A. Marquette, A. Degiuli and L. c. J. Blum, *Biosens. Bioelectron.*, 2003, **19**, 433-439.
35. B. P. Corgier, C. A. Marquette and L. J. Blum, *Anal. Chim. Acta*, 2005, **538**, 1-7.
36. K.-J. Huang, D.-J. Niu, W.-Z. Xie and W. Wang, *Anal. Chim. Acta*, 2010, **659**, 102-108.
37. Z. Wang, X. Hao, Z. Zhang, S. Liu, Z. Liang and G. Guan, *Sens. Actuators, B*, 2012, **162**, 353-360.
38. M. Zhang and W. Gorski, *J. Am. Chem. Soc.*, 2005, **127**, 2058-2059.

- 1 39. H. Ye, H. Xu, X. Xu, C. Zheng, X. Li, L. Wang, X. Liu and G. Chen,  
2 *Chem. Commun.*, 2013, **49**, 7070-7072.
- 3 40. Y. Liu, M. Wang, F. Zhao, Z. Xu and S. Dong, *Biosens. Bioelectron.*,  
4 2005, **21**, 984-988.
- 5 41. D. C. Duffy, J. C. McDonald, O. J. Schueller and G. M. Whitesides,  
6 *Anal. Chem.*, 1998, **70**, 4974-4984.
- 7 42. W. Suginta, P. Khunkaewla and A. Schulte, *Chem. Rev.*, 2013, **113**,  
8 5458-5479.
- 9 43. S. B. Zhang, Z. S. Wu, M. M. Guo, G. L. Shen and R. Q. Yu, *Talanta*,  
10 2007, **71**, 1530-1535.